132 kV optical voltage sensor for wide area monitoring, protection and control applications

Grzegorz Fusiek, Pawel Niewczas
University of Strathclyde
Glasgow, UK
g.fusiek@strath.ac.uk

Neil Gordon, Philip Orr
Synaptec
Glasgow, UK
neil.gordon@synapt.ec

Paul Clarkson
National Physical Laboratory
London, UK
paul.clarkson@npl.co.uk

Abstract— This paper reports on the design, construction and initial testing of a fiber-optic voltage sensor for applications in the field of wide area monitoring, protection and control of high voltage power networks. The 132-kV sensor prototype, combining a capacitive voltage divider (CVD) and an optical low voltage transducer (LVT), was evaluated through laboratory testing and its performance was assessed based on the accuracy requirements specified by the IEC standards for low-power passive voltage transformers. The preliminary results show that the device has the potential to comply with the requirements of the 0,2 class for metering devices, and the 3P and 0,5P classes for protective and multipurpose devices, respectively, as specified by IEC 61869-11. As the device is based on a fiber Bragg grating written in a standard, low-loss, single-mode telecommunication fiber, it has the potential to be deployed as part of a distributed network of sensors along the power network over a wide geographical area, enabling novel power system protection and control strategies.

Keywords— Fiber Bragg grating, optical voltage sensor, power system instrumentation, capacitive voltage divider

I. INTRODUCTION

Wide Area Monitoring, Protection and Control (WAMPAC) systems have become a promising solution to improve the performance of the electrical power networks. By ensuring the increased network visibility and fast reaction to the network demands and disturbances, WAMPAC aims at a significant reduction in the number of blackouts and improvements in the power networks reliability and security [1]-[3].

Conventional instrument transformers together with phasor measurement units (PMUs) are important components of the WAMPAC systems. Although conventional iron-core current transformers (CTs) and voltage transformers (VTs) remain the dominant technology in the energy sector to monitor transmission network parameters, they suffer from heavy weight, large size, lack of galvanic isolation and core saturation problems as well as pose risks of explosion causing safety issues [4]. As an alternative to conventional CTs and VTs, the optical voltage transducers (OVTs) based on Pockels effect and optical current transducers (OCTs) based on Faraday effect have been proposed [5]-[7]. In contrast to CTs and VTs, they offer a number of benefits such as light weight, small size, wide bandwidth, high accuracy, immunity to electromagnetic interference and galvanic isolation. However, the commercial uptake of this technology has been slow due to the high cost of the optical instrumentation solutions based on polarimetry, its vulnerability to temperature and vibration effects [7], and the reticence of the power industry to adopt new technologies. Importantly, while the conventional OCTs and OVTs may offer a direct replacement for CTs and VTs, they are incapable of being deployed passively over long distances to offer passive WAMPAC. Therefore, novel sensor systems capable of providing distributed voltage and current measurement while remaining cost competitive with current technology are required as part of the developing WAMPAC technologies.

To enable access to multiple, remote, distributed, passive current and voltage measurements over long distances that can be applicable to a wide range of metering and protection applications and to provide novel power system protection functions that are not possible with current technology, the concept of a photonic sensors suite utilizing fiber Bragg grating (FBG) sensors was proposed by the authors [8]. We previously developed an optical current sensor (OCS) for protection applications and evaluated its performance according to the relevant industry standards [9]. The core technology utilised in the current sensors was based on a Low Voltage Transducer (LVT), which could be interfaced directly with a Rogowski coil or, through a burden resistor, with a conventional CT to enable current measurements. We showed that the prototype OCS was capable to meet the accuracy requirements of the 5P class. We also recently developed an optical voltage sensor (OVS) for medium voltage (MV) networks (11 kV) [10]. The device was capable of providing voltage measurements with accuracy better than 0.2 %, showing the potential of meeting the requirements of the 3P protection and 0,2 metering classes.

In this paper, we concentrate on the design, construction and preliminary evaluation of a prototype OVS for high voltage networks to assess its potential to comply with the combined IEC metering and protection standards. Details of sensor design and construction and the selection of components and packaging are proposed in order to ensure compliance with the metering and protection classes and safety requirements applicable to 132 kV networks. The device performance is verified according to IEC 61869-11 for low-power passive voltage transformers as the most relevant standard [11].

II. OPTICAL VOLTAGE SENSOR DESIGN

A. Design requirements

The proposed optical voltage sensor was designed to be connected between one line of a 50-Hz 132-kV system and

Research presented in this paper was supported by the Innovate UK (project number 102594 and 109487-627607) and the UK Engineering and Physical Sciences Research Council (grant reference EP/P510300/1). All data underpinning this publication are openly available from the University of Strathclyde KnowledgeBase at https://doi.org/10.15129/475d0933-180f-45dc-8d32-a136ab52ef07

earth, and its rated voltage is equal to 80 kV with the rated voltage factor of 1.2 applicable to measurements between phase and earth on a continuous basis [11]. Additionally, the device must withstand the rated power-frequency voltage of 275 kV and the rated lightning-impulse voltage of 650 kV [12].

B. Low voltage transducer

The LVT, shown in Fig. 1, comprises a low-voltage piezoelectric multilayer stack and a bonded fiber Bragg grating (FBG) sensor [9], [13].

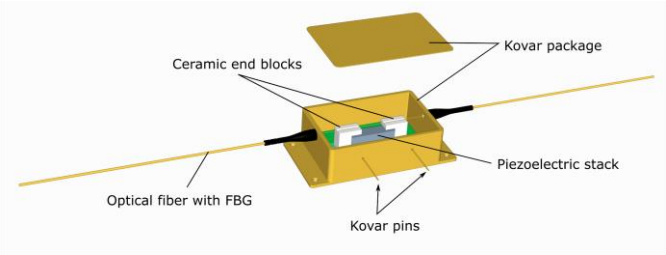

Fig. 1. Low voltage transducer.

In the proposed design, the FBG sensor was suspended between two ceramic arms attached to a rectangular block of PICMA® stack from Physik Instrumente (PI) [14]. The stack has nominal dimensions 5×5×18 mm and its operating voltage range is from -30 V to 120 V. It has a resonant frequency of 135 kHz and can reach its full displacement in approximately 2.5 µs after the driving voltage change.

The transducer is housed in a telecommunication industry standard, hermetically sealed butterfly package. Voltage input to the piezoelectric stack is provided through two Kovar pins isolated from the package, as shown in Fig. 1. Strain proportional to the input voltage is imparted to the FBG by the piezoelectric stack. The sensor can be interrogated remotely by measuring the peak wavelength reflected by the FBG, which shifts in proportion to the strain and hence applied voltage due to the change in period of the grating. By tracking the instantaneous peak wavelength, the voltage input can be reconstructed, and by tracking the average wavelength, local sensor temperature can be derived that can be used for temperature compensation of the sensor voltage readings [9], [10], [13].

The LVT construction ensures strain amplification [13], and its operating voltage range is limited to ±30 V by means of an external protection circuitry formed by a protection resistor (R_p) and a bidirectional transient-voltage-suppression (TVS) diode (see Fig. 2) to avoid the piezoelectric component depolarization and permanent damage. The LVT has been designed with the requirements of environmental isolation, long-term reliability and potential for mass production in mind.

C. Capacitive voltage divider

The proposed configuration for an HV capacitive voltage divider is shown in Fig. 2. The role of the capacitive voltage divider is to reduce the high voltage to the low level that can normally be handled by the LVT, eliminating the need for excessive insulation. To bring the voltage down from ~100 kV to ~20 V (RMS), the voltage division ratio of 5000 was chosen. Assuming the LVT capacitance of 1.5 µF, the practical values of capacitors C_1 and C_2 were chosen as 1 nF and 3.5 µF, respectively.

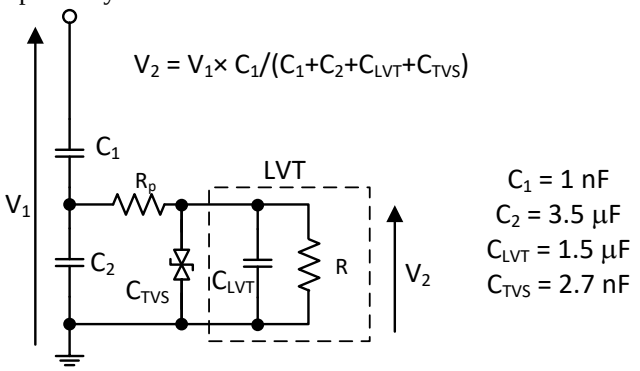

Fig. 2. HV divider diagrams: LVT measuring output voltage of a HV-to-LV divider. The dividing ratio is 5000 assuming the LVT capacitance of 1.5 µF.

D. HV sensor construction

The prototype HV sensor construction is shown in Fig. 3. In the proposed design, the LVT is combined with a CVD as described in the previous section.

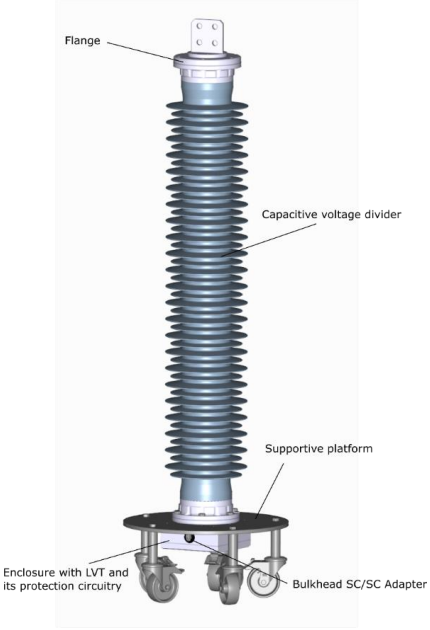

Fig. 3. Optical voltage sensor for HV networks.

The bespoke CVD is housed in a single HV composite insulator and was provided by an external supplier (CONDIS SA). To offer access to the low voltage output, the divider is interfaced with the LVT placed in a die-cast enclosure at ground level, and the access to the CVD low voltage terminal is provided inside the enclosure. The laboratory prototype is mounted on a platform with swivel wheels to allow for easy transportation.

The CVD underwent successfully tests against the power frequency and lightning impulse withstand voltages and partial discharge tests, meeting the IEC standard requirements.

III. ACCURACY CLASS REQUIREMENTS

For protection class devices, the maximum voltage and phase errors at the rated frequency are specified in TABLE I [11].

TABLE I. PROTECTION CLASS ACCURACY REQUIREMENTS

Accuracy class	Ratio error ε, $\varepsilon_{cor\,U}$ ± %					Phase error φ_e, $\varphi_{cor\,\varphi o}$ ± minutes					Phase error φ_e, $\varphi_{cor\,\varphi o}$ ± centiradians				
	at voltage (% of rated)					at voltage (% of rated)					at voltage (% of rated)				
	2	20	80	100	F_V x100	2	20	80	100	F_V x100	2	20	80	100	F_V x100
0,1P	0,5	0,2	0,1	0,1	0,1	20	10	5	5	5	0,6	0,3	0,15	0,15	0,15
0,2P	1	0,4	0,2	0,2	0,2	40	20	10	10	10	1,2	0,6	0,3	0,3	0,3
0,5P	2	1	0,5	0,5	0,5	80	40	20	20	20	2,4	1,2	0,6	0,6	0,6
1P	4	2	1	1	1	160	80	40	40	40	4,8	2,4	1,2	1,2	1,2
3P	6	3	3	3	3	240	120	120	120	120	7	3,5	3,5	3,5	3,5
6P	12	6	6	6	6	480	240	240	240	240	14	7	7	7	7

For metering class devices, the voltage and phase errors at the rated frequency should not exceed the values specified in TABLE II at any voltage between 80 % and 120 % of the rated voltage [11].

TABLE II. METERING CLASS ACCURACY REQUIREMENTS

Accuracy class	Percentage ratio error ε, $\varepsilon_{cor\,U}$ ± %			Phase error φ_e, $\varphi_{cor\,\varphi o}$ ± Minutes			Phase error φ_e, $\varphi_{cor\,\varphi o}$ ± Centiradians		
	at voltage (% of rated)			at voltage (% of rated)			at voltage (% of rated)		
	80	100	120	80	100	120	80	100	120
0,1	0,1	0,1	0,1	5	5	5	0,15	0,15	0,15
0,2	0,2	0,2	0,2	10	10	10	0,3	0,3	0,3
0,5	0,5	0,5	0,5	20	20	20	0,6	0,6	0,6
1,0	1,0	1,0	1,0	40	40	40	1,2	1,2	1,2
3,0	3,0	3,0	3,0	Not specified			Not specified		

Additionally, the accuracy needs to be verified at the rated voltage and at frequencies equal to 96 % and 102 % of the rated frequency, which is the requirement for protection class devices, and at frequencies equal to 99 % and 101 % of the rated frequency, which is the requirement for metering class devices [12].

IV. EXPERIMENTAL RESULTS

A. Experimental setup

A schematic diagram of the experimental setup is shown in Fig. 4. The HV OVS calibration is performed using a comparison method specified by IEC 60060-2 [15]. The device under test (DUT) is connected in parallel with a voltage reference system, and calibrated by the comparison of both measurement system outputs.

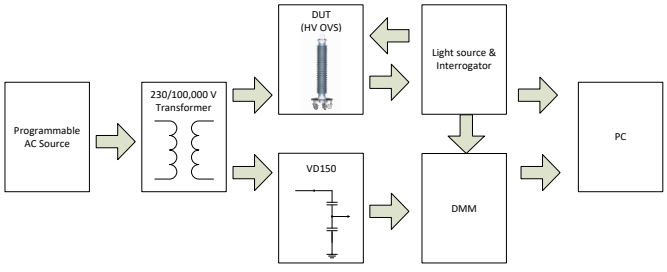

Fig. 4. Schematic diagram of the experimental setup.

The test voltage is provided from a step-up transformer capable of delivering up to 100 kV. The transformer is powered from a programmable AC source, Chroma 61512, capable of delivering 18 kVA at 300 V. The voltage reference signal is obtained from a voltage divider, VD150 (Ross Engineering) [16], providing the nominal 14000:1 voltage division ratio. The unit is suitable for measuring DC and AC voltages up to 150 kV. The VD150 output is monitored by a Keysight 3458A digital multimeter (DMM) connected to a PC via USB/GPIB cable and isolated from a PC via an optical USB cable.

A photograph of the high voltage calibration and testing facility at Strathclyde is shown in Fig. 5. During the calibration and accuracy testing, the optical sensors are illuminated by a broadband light source and the reflected signals can be analyzed using an FBG interrogator. In the current embodiment of the system, an I-MON 256 USB (Ibsen Photonics) connected to a PC is used. However, it is possible to use different interrogation systems that can provide a clock signal to synchronize data acquisition from the interrogator with that of the DMM. The optical system clock in I-MON (4 kHz) is used to synchronize the interrogator readings with the DMM readings. The clock signal from I-MON is provided to the DMM via a dedicated optical link.

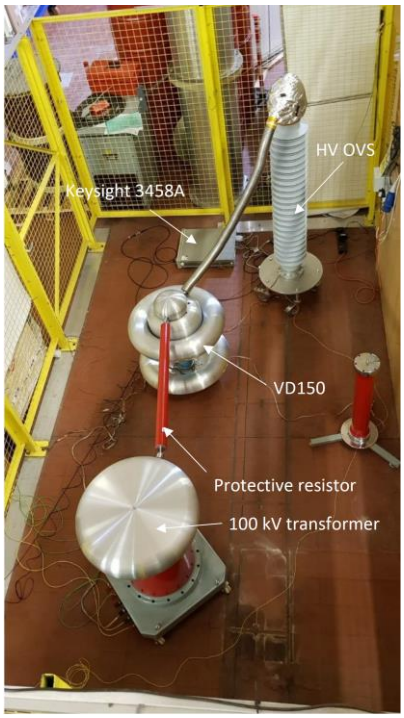

Fig. 5. Experimental setup.

In the current system implementation, provision of an additional trigger that would release both systems at the same time was not possible. While data samples from both systems can be acquired at the same time and synchronized, the acquisition of the sensor and reference signals starts at different moments each time the software controlling acquisition is started, causing a random phase displacement between the acquired signals. Therefore, the sensor phase calibration is not possible at the moment and only amplitude calibration can be

performed. This, however, will be improved as soon as the new generation interrogator capable of delivering an external trigger is available.

B. *Independent calibration of the voltage reference system*

In addition to the manufacturer's calibrations, the voltage reference system comprising the VD150 and Keysight 3458A, was calibrated at the Research Institutes of Sweden (RISE) [17] in the following measurement conditions: room temperature 22 °C ± 2 °C; frequency 50 Hz ± 0.1 Hz.

The relationship between the VD150 scale factor and the applied primary voltage is shown in Fig. 6. The divider scale factor values for AC measurements were calibrated with the extended uncertainty of ±0.02 % (coverage factor k = 2, confidence level 95 %). A second order polynomial was fitted into the data and used for the sensor calibration described in the next section.

In short-term measurements (hours), the relative change of the scale factor with voltage was shown to be below 0.05 %. On the day-to-day basis, the system complied with the accuracy of 0.2 %.

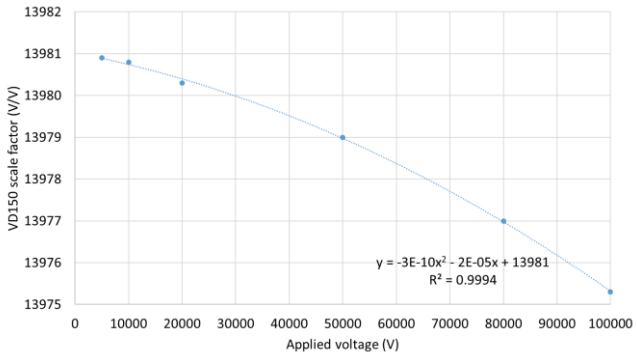

Fig. 6. VD150 scale factor versus applied voltage based on the equipment calibration at RISE, Sweden.

C. *Sensor calibration*

The voltage characterization of the sensor was performed in laboratory conditions at room temperature (21 ± 1 °C) according to the IEC 60044-7 requirements [12].

To calibrate the HV OVS, a 50 Hz sinusoidal voltage was applied to the sensor at 2 %, 5 %, and in the range from 10 % to 120 % of the nominal voltage (80 kV) in 10 % increments. The readings of the optical signals from the sensor and the readings from the DMM were logged together at each voltage level as described above.

At each voltage level, 8000 samples, equivalent to 100 periods of 50 Hz signals, were captured. The rms values were then calculated from 10 periods for 10 measurements at each voltage level as per IEC60060-2 [15]. The rms calculations were performed for the main frequency components of the signals using FFT analysis.

To convert the DMM output voltage (0-10 V range) to the primary voltage level, the interpolated values of the VD150 scale factor as a function of primary voltage were used.

To create the sensor calibration curve, shown in Fig. 7, a fourth order polynomial was fitted into the data obtained from the first characterization run. The errors due to the goodness of fit and the associated uncertainties were below 0.002, an order of magnitude lower than the uncertainties associated with the VD150 stability and scale factor estimation. Therefore, they can be neglected.

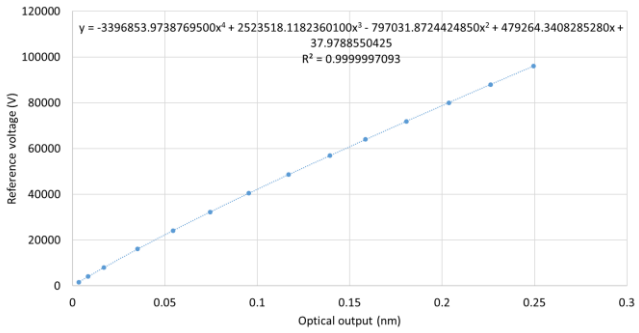

Fig. 7. HV OVS calibration curve.

The sensor calibration equation, shown in Fig. 7, was then implemented in software and used to convert the FBG peak wavelength shifts into the measured primary voltage levels.

D. *Accuracy tests*

To assess the suitability of the sensor for protection and metering purposes, 50 Hz voltage waveforms with amplitudes of 2 %, 20 % and between 80 % and 120 % of the device rated voltage were applied as part of the test procedure. For each case, the measurements were repeated three times.

The amplitude errors were calculated according to the following equation:

$$\varepsilon(\%) = \frac{V_p - V_{rec}}{V_p} \cdot 100 \qquad (1)$$

where V_p is the rms value of primary voltage and V_{rec} is the rms value of the reconstructed voltage [11], [12].

The voltage errors for the combined three consecutive test runs are shown in Fig. 8.

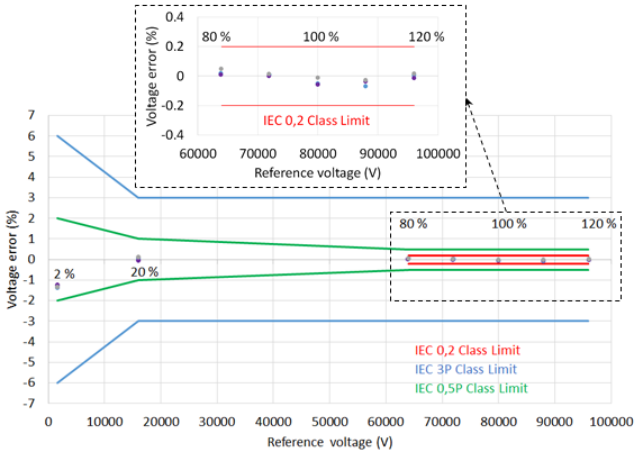

Fig. 8. HV OVS voltage errors for three consecutive test runs.

As indicated previously in TABLE I. and TABLE II., for the IEC 0,2 metering class, the voltage errors at the rated frequency

should not exceed 0.2 % at any voltage between 80 % and 120 % of the rated voltage (64 kV and 96 kV, respectively). The HV OVS voltage errors are significantly lower than the limits set by the standard. For the 3P class protective devices, the voltage errors at 20 % of the nominal voltage (16 kV) and between 80 % and 120 % of the rated voltage (at 1.2 voltage factor for this sensor) the voltage error should be below 3 %. At 2 % of the nominal voltage (1.6 kV) it should be below 6 %. Clearly, the HV OVS performance is better than the requirements set by the standard with the amplitude errors below 1.4 % at 2 % of the rated voltage, and 0.2 % at 20 % and between 80 % and 120 % of the nominal voltage, respectively. In addition, for multipurpose devices, the requirements for the amplitude errors at 2 %, 20 %, and between 80% and 120 % of the rated voltage should be below 2 %, 1 % and 0.5 %, respectively, for the 0,5P class. Clearly, the device meets these requirements as well.

The next experiment involved testing the sensor performance at the rated voltage and at frequencies equal to 96 % and 102 % of the rated frequency, which is the requirement for protection class devices, and at frequencies equal to 99 % and 101 % of the rated frequency, which is the requirement for metering class devices. For the nominal frequency of 50 Hz, this is equivalent to 48 Hz and 51 Hz, and 49.5 Hz and 50.5 Hz, respectively. The results of three combined test runs are presented in Fig. 9. The amplitude errors are less than 0.2 %, which satisfies the requirements for both the IEC 3P protection and 0,2 metering classes. Thus, a single device has the potential to meet the 3P protection and 0,2 metering classes.

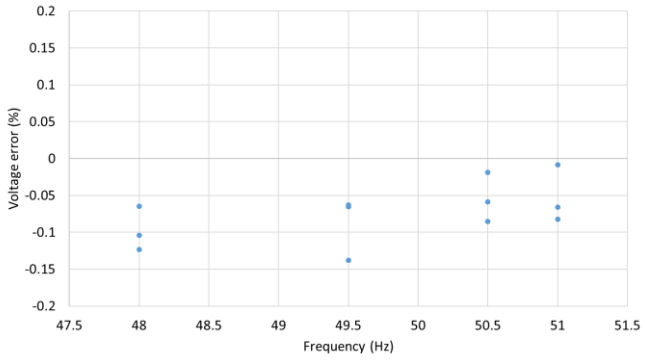

Fig. 9. HV OVS errors at nominal voltage and frequencies of 48 Hz, 49.5 Hz, 50.5 Hz, and 51 Hz as specified by the combined IEC 3P protection and 0,2 metering classes.

As indicated earlier, the sensor phase calibration, and hence, phase errors estimation was not possible due to the current implementation of the sensor calibration system. However, based on the Bode analysis of the HV OVS circuitry (shown in Fig. 2), the expected phase displacement between the primary voltage and the voltage across the LVT is below 7 minutes assuming R_p = 5 Ω and R = 200 MΩ [14], thus having the potential to meet the 0,2, 0.5P and 3P class requirements. The phase errors will be confirmed experimentally as soon as the improved calibration system is available in the future.

V. Conclusions

In this paper, the design and construction of an optical voltage sensor for distributed voltage measurements on high-voltage networks (132 kV) has been presented. The sensor performance was evaluated against the IEC 61869-11 standard. The preliminary results of the accuracy tests have shown that the sensor has the potential to meet the requirements of the IEC 0,2 class for metering devices, 3P and 0,5P classes for protective and multipurpose devices.

Future work will focus on performing additional tests, such as temperature, routine and special tests according to the relevant standards and verifying the sensor phase errors and long-term performance.

References

[1] V. Terzija *et al*., "Wide-Area Monitoring, Protection, and Control of Future Electric Power Networks," in *Proceedings of the IEEE*, vol. 99, no. 1, pp. 80-93, Jan. 2011.

[2] A. G. PHADKE, P. WALL, L. DING, and V. TERZIJA, "Improving the performance of power system protection using wide area monitoring systems," *J. Mod. Power Syst. Clean Energy*, vol. 4, no. 3, pp. 319–331, Jul. 2016.

[3] A. Vaccaro, A. F. Zobaa, "Wide area monitoring, protection and control systems: the enabler for smarter grids", IET, 2016

[4] T. Bi, H. Liu, X. Zhou and Q. Yang, "Impact of transient response of instrument transformers on phasor measurements," *IEEE PES General Meeting*, Providence, RI, 2010, pp. 1-6.

[5] K. Bonhert, P. Gabus, J. Kostovic and H. Brändle "Optical fiber sensors for the electric power industry," Opt. Lasers Eng., vol 43, pp. 511-526, 2005.

[6] L. Bi and H. Li, "An Overview of Optical Voltage Sensor," 2012 International Conference on Computer Science and Electronics Engineering, Hangzhou, 2012, pp. 197-201.

[7] Silva, R.M.; Martins, H.; Nascimento, I.; Baptista, J.M.; Ribeiro, A.L.; Santos, J.L.; Jorge, P.; Frazão, O. Optical Current Sensors for High Power Systems: A Review. *Appl. Sci.* **2012**, *2*, 602-628.

[8] P. Orr, G. Fusiek, P. Niewczas, C. Booth, A. Dyśko, F. Kawano, T. Nishida, P. Beaumont, "Distributed Photonic Instrumentation for Power System Protection and Control" IEEE Transactions on Instrumentation and Measurement journal, 64(1) 2015

[9] J. Nelson, G. Fusiek, L. Clayburn, P. Niewczas, C. Booth, P. Orr, N. Gordon, "Development and testing of optically-interrogated current sensors", AMPS 2016

[10] G. Fusiek, J. Nelson, P. Niewczas, J. Havunen, E. Suomalainen and J. Hällström, "Optical voltage sensor for MV networks," *2017 IEEE SENSORS*, Glasgow, 2017, pp. 1-3.

[11] IEC 61869, "Instrument transformers – Part 11: Additional requirements for low-power passive voltage transformers", 2017

[12] IEC 60044, "Instrument transformers – Part 7: Electronic voltage transformers", 1999

[13] G. Fusiek, P. Niewczas, M. Judd, "Towards the Development of a Downhole Optical Voltage Sensor for Electrical Submersible Pumps", Sensors and Actuators A: Physical, Volume 184, September 2012, Pages 173-181, ISSN 0924-4247

[14] Physik Instrumente Ltd website, available at: http://www.piceramic.com

[15] IEC 60060, "High-voltage test techniques – Part 2: Measuring Systems,", 2011

[16] Ross Engineering Corporation, website, available at: https://www.rossengineeringcorp.com

[17] RISE Research Institutes of Sweden, website, available at: http://www.sp.se